
Volume 310 Issue 10 1 May 2008 ISSN 0022-0248
ELSEVIER
JOURNAL OF CRYSTAL GROWTH
EDITORS:
T.F. KUECH (Principal Editor), University of Wisconsin-Madison
M. SCHIEBER (Founding Editor), Hebrew University
R.S. FEIGELSON, Stanford University
R. KERN, Univ. Aix-Marseille
K. NAKAJIMA, Tohoku University
G.B. STRINGFELLOW University of Utah
CO-FOUNDERS: N. CABRERA, B. CHALMERS, F.C. FRANK
FORMER ADVISOR: R.A. LAUDISE†
Available online at
ScienceDirect
www.sciencedirect.com

Available online at www.sciencedirect.com
ScienceDirect
ELSEVIER
Journal of Crystal Growth 310 (2008) 2476–2479
JOURNAL OF CRYSTAL GROWTH
www.elsevier.com/locate/jcrysgro

Nitride-based light-emitter and photodiode dual function devices with InGaN/GaN multiple quantum dot structures

L.W. Ji[a,*], S.J. Young[b], C.H. Liu[a], W. Water[c], T.H. Meen[c], W.Y. Jywe[a]

[a]Institute of Electro-Optical and Materials Science, National Formosa University, Yunlin 632, Taiwan, ROC
[b]Institute of Microelectronics & Department of Electrical Engineering, National Cheng Kung University, Tainan 70101, Taiwan, ROC
[c]Department of Electronic Engineering, National Formosa University, Yunlin 632, Taiwan, ROC

Received 8 October 2007; received in revised form 22 October 2007; accepted 10 January 2008
Communicated by M. Schieber
Available online 30 January 2008

Abstract

In this work, a light-emitter with InGaN/GaN multiple quantum dot structures has been employed for a dual function device exhibiting the photodiode (PD) characteristics in reverse bias. The turn-on voltage in forward bias and the breakdown voltage in reverse bias were 3 and −13.5 V, respectively. Furthermore, with an incident wavelength of 350 nm and 3 V applied bias, the maximum responsivity of this device was 0.13 A/W. It was also found that the responsivity was nearly a constant from 390 to 440 nm. Thus, one can easily integrate PDs with LEDs using the same epistructure to realize a GaN-based optoelectronic integrated circuit.

Keywords: A1. Nanostructures; B2. Semiconducting II–VI materials; B3. Light-emitting diodes

1. Introduction

Highly strained material systems with heteroepitaxial growth have been quite attractive that it offers the possibility of producing low-dimensional carrier confinement nanostructures, such as quantum wells and quantum dots [1]. III-Nitride with wurtzite crystal structure is a direct energy bandgap semiconductor. We could also achieve nitride-based heteroepitaxial growth easily. At room temperature, the bandgap energy of AlInGaN varies from 0.7 to 6.2 eV depends on its composition. Therefore, nitride-based semiconductor materials have been intensively studied as prospective candidates for wide bandgap optical devices such as light-emitting diodes (LEDs) and laser diodes (LDs) [2,3]. Typical high-brightness LEDs have a multiple quantum well active region. The multiple quantum well LED is a kind of heterojunction device, in which electrons and holes are confined in the well layers. Thus, one can achieve high quantum efficiency from the multiple quantum well LEDs since carrier can recombine easily in the confined well layers [4,5]. Although high brightness InGaN–GaN multiple quantum well LEDs are already commercially available, it can be theoretically predicted that the realization of LEDs with quantum dots in the active layer would improve the performance of LEDs.

Lately, it has been shown that nitride nanostructures can be self-assembled using the strain-induced Stranski–Krastanov (S–K) growth mode without any substrate patterning process [6–8]. It has also been shown that nitride nanostructures can be self-assembled using growth interruption during the metal–organic chemical vapor deposition (MOCVD) growth [9,10]. Although the size fluctuations of self-assembled quantum dots could result in inhomogeneous optical and electrical characteristics, the self-assembly of strain-induced islands provides the means for creating quasi-zero-dimensional quantum structures without having to overcome the current limitations of lithography. These self-assembled quantum dots could also be used to study novel device physics [11–13].

In this work, we employed a InGaN/GaN multiple quantum dot structure in LEDs for achieving dual-function

*Corresponding author. Tel.: +886 5 631 5679; fax: +886 5 632 9257.
E-mail addresses: lwji@seed.net.tw, lwji@nfu.edu.tw (L.W. Ji).

0022-0248/$ - see front matter © 2008 Elsevier B.V. All rights reserved.
doi:10.1016/j.jcrysgro.2008.01.028

optoelectronic devices exhibiting photodiode (PD) properties in reverse bias, while at the same time preserving the distinct identities of LED under forward bias. In addition, we discuss the optoelectronic characteristics (including electroluminescence (EL) and current–voltage measurements) of the InGaN–GaN multiple quantum dot LEDs compared with conventional multiple quantum well LEDs. Thus, one can easily integrate PDs with LEDs using the same structure to realize a GaN-based optoelectronic integrated circuit.

2. Experiment

Samples used in this study were grown on (0 0 0 1)-oriented 2-inch sapphire (Al_2O_3) substrates in a vertical low-pressure MOCVD reactor with a high-speed rotation disk [4,5]. Briefly, the gallium, indium and nitrogen sources were trimethylgallium (TMGa), trimethylindium (TMIn), and ammonia (NH_3), respectively. Biscyclopentadienyl magnesium (CP_2Mg) and disilane (Si_2H_6) were used as the p- and n-type doping sources, respectively.

Prior to growth, sapphire substrates were thermally baked at 1100 °C in hydrogen gas to remove surface contamination. After a 30-nm-thick low-temperature GaN nucleation layer was deposited onto the sapphire substrate at 500 °C, the temperature was raised to 1000 °C to grow the Si:GaN buffer layer. Subsequently, the temperature was ramped down to 730 °C to grow the InGaN–GaN multiple quantum well active region with InGaN QDs. It should be noted that we introduced an interrupted growth method [9,10] so as to achieve the multiple quantum dot structures. In the multiple quantum dot region, each InGaN/GaN pair consists a 2.4-nm-thick InGaN well layer and a 15-nm-thick GaN barrier layer. After the growth, the surfaces of the as-grown samples were partially etched until the n-type GaN layers were exposed. Ni–Au contacts were subsequently evaporated onto the p-type GaN surfaces to serve as the p-electrodes, and Ti–Al–Ti–Au contacts were deposited onto the exposed n-type GaN layers to serve as the n-type electrodes, to complete the fabrication of the InGaN/GaN multiple quantum dot dual function devices.

For structural characterization, the cross-sectional transmission electron microscopy (XTEM) was employed for TEM observation. For the fabricated devices, room temperature EL characteristics were also measured by injecting current into these samples. Room temperature current–voltage (*I–V*) characteristics of the devices were then measured by an HP 4145 semiconductor parameter analyzer under both dark and illumination. The top-illuminated spectral responsivity of these devices was also quantified using a Xe arc lamp with a calibrated monochromator as the light source. The monochromatic light, calibrated with UV-enhanced Si photodetectors and an optical power meter, was collimated onto each photodetector via an optical fiber.

3. Results and discussion

As shown in Fig. 1, the XTEM image of multiple quantum dot structures in p–n junction dual function devices was taken along the GaN [1 1 2 0] direction and the dark-field image was obtained under two beam condition with $g = [0\,0\,0\,2]$. We can achieve nanoscale self-assembled quantum dots by using the growth interruption method during MOCVD growth [13], it can be seen that there are obvious dots-in-a-well (DWELL) structures in the active region. The density of these quantum dots was estimated to range between 10^{10} and $10^{11}\,cm^{-2}$ [9,10]. Since all the quantum dots exist in the well layer, the formation mechanism of quantum dots in this specimen should be strain-induced S–K epitaxial growth, not phase separation. III–V Nitride heterostructures have a large piezoelectric effect along the [0 0 0 1] orientation, especially in strain-induced self-assembled quantum dot structures. As a result, we can predict such a DWELL structure will reveal strong quantum localization effect.

Fig. 2 shows current–voltage (*I–V*) characteristics of the multiple quantum dot LEDs and conventional multiple quantum well LEDs fabricated using similar process sequences, the 20 mA forward voltage is 3.1 and 3.5 V, respectively. The smaller forward voltage 3.1 V shows better electrical performance on the fabricated multiple quantum dot LEDs, it may be attributed to quantum dots are effective in reducing the forward voltage due to the 3-D spatial confinement effect of carriers. In this work, we can see that DWELL structures effectively lowered the operating voltage of LEDs.

Fig. 3 shows room temperature EL spectra of the fabricated multiple quantum dot LED with various DC

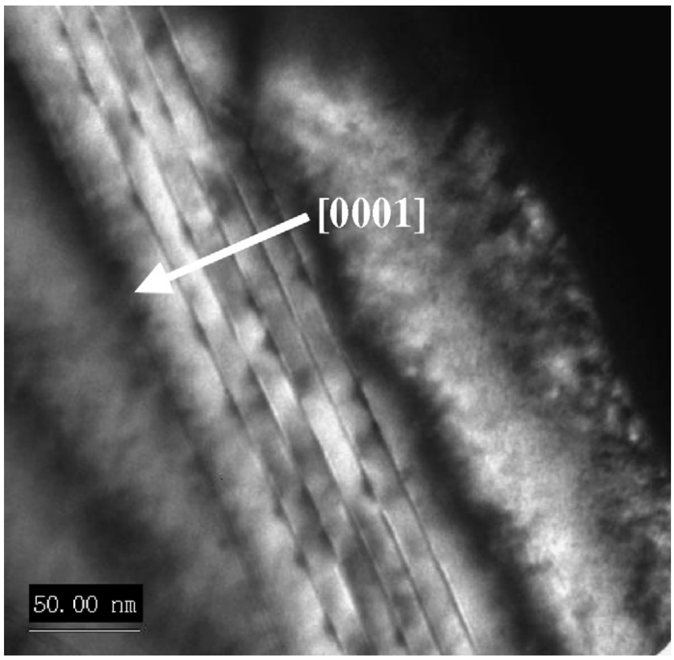

Fig. 1. XTEM picture of InGaN/GaN multiple quantum dot structure.

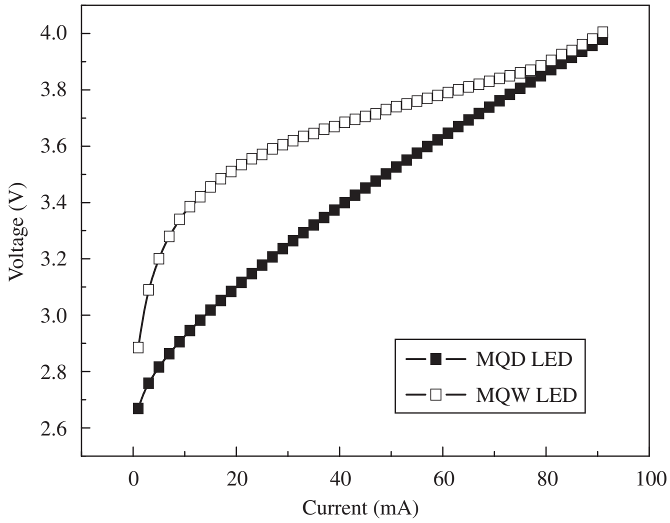

Fig. 2. Current–voltage (*I*–*V*) characteristics of the multiple quantum dot LEDs and multiple quantum well LEDs, the forward voltage and EL intensity is 3.1 and 3.5 V at 20-mA injection current, respectively.

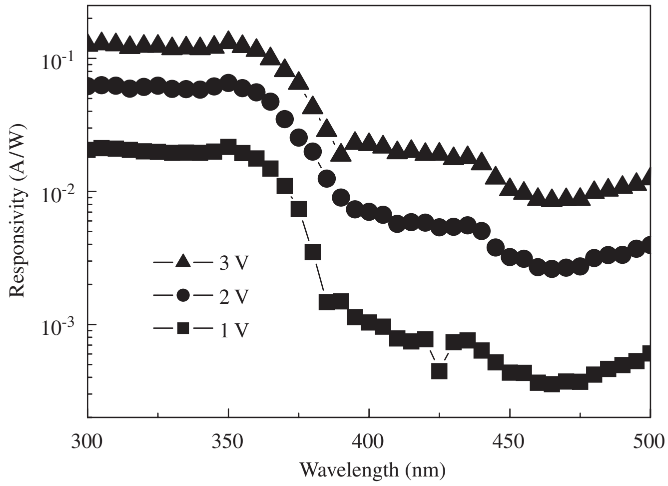

Fig. 4. Spectral response measured at applied bias 1, 2, and 3 V.

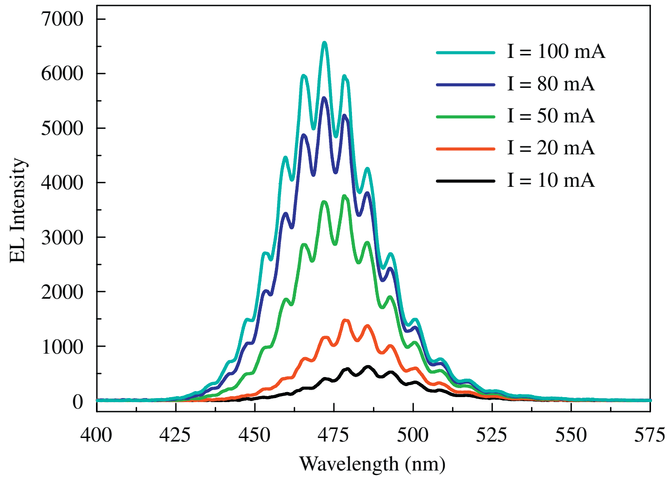

Fig. 3. Room temperature EL spectra with different forward injection current for multiple quantum dot LED.

injection currents. It was found that EL is blue-shifted as DC injection current increases. It was also found that the EL spectrum shows a pronounced undulation. This undulation behavior is probably due to the Fabry–Perot interferences within the epitaxial layers [14].

We have ever observed a huge 68.4-meV EL blue shift as the injection current was increased for multiple quantum dot LED. Such a value is much more than the 38-meV EL blue shift observed from conventional nitride-based multiple quantum well LED with a similar structure in the same current range [15]. It is well-known that III–V nitride materials have a large piezoelectric effect, especially in strain-induced self-assembled quantum dot structures. The large piezoelectric field will induce quantum-confined Stark effect [16,17]. Quantum-confined Stark effect results in a spatial separation of electrons and holes, and thus, the carrier recombination energy will become smaller. In this study, since quantum dot structures have stronger quantum-confined Stark effect, the large EL blueshift reveals that deep localization of excitons (or carriers) originates from quantum dots will strengthen band-filling effect as the injection current increases. Furthermore, a blue shifts due to the quantum size effect should be also noticeable. It should be noted that strain-induced III-nitride self-assemble quantum dots will result in quantum-confined Stark effect, is very different from the other non-hexagonal semiconductor self-assemble quantum dots. Hence the large EL variation in quantum dot LED can be expected in this work.

The room temperature spectral response of p–n junction multiple quantum dot PDs under various applied bias voltage was shown in Fig. 4. With an incident wavelength of 350 nm and 3 V applied bias, the maximum responsivity of this device was 0.13 A/W. Moreover, it was also found that the responsivity was nearly a constant from 390 to 440 nm. Furthermore, the peak responsivity of our device also increase with the applied bias, which indicates the possibility of internal gain. Here, we define UV to visible rejection ratio as the responsivity measured at 350 nm over the responsivity measured at 465 nm. With this definition, the UV to visible rejection ratio at 1 V bias were estimated to be 56. Such high responsivity and rejection ratio of our device suggest that our sample is very suitable for the light detection in the ultraviolet region [18].

4. Summary

In summary, an InGaN/GaN multiple quantum dot structure used for LEDs has been employed for dual functions of optoelectronic devices exhibiting photodetector properties in reverse bias, while at the same time preserving the distinct identities of LED in forward bias. The turn-on voltage in forward bias and the breakdown voltage in reverse bias were about 3 and −13.5 V, respectively. Furthermore, with an incident wavelength of 350 nm and 3 V applied bias, the maximum responsivity of this device was 0.13 A/W. It was also found that the responsivity was nearly a constant from 390 to 440 nm. It seems to suggest that the spectral response in the range of 390–440 nm is due to the effect of the InGaN dots-in a well active layers. Thus, one can easily integrate photodetectors with LEDs using the same epistructure to realize a GaN-based optoelectronic integrated circuit.

Acknowledgment

This work was supported by National Science Council under Contract number NSC-95-2221-E-150-077-MY3.

References

[1] D. Leonard, M. Krinshnamurthy, C.M. Reaves, S.P. Denbaars, P.M. Petroff, Appl. Phys. Lett. 63 (1993) 3203.
[2] F.A. Ponce, D.P. Bour, Nature 386 (1997) 351.
[3] S. Nakamura, Science 281 (1998) 956.
[4] Y.K. Su, S.J. Chang, C.H. Ko, J.F. Chen, W.H. Lan, W.J. Lin, Y.T. Cherng, J. Webb, IEEE Trans. Electron. Dev. 49 (2002) 1361.
[5] L.W. Wu, S.J. Chang, T.C. Wen, Y.K. Su, W.C. Lai, C.H. Kuo, C.H. Chen, J.K. Sheu, IEEE J. Quantum Electron. 38 (2002) 446.
[6] B. Damilano, N. Grandjean, S. Dalmasso, J. Massies, Appl. Phys. Lett. 75 (1999) 3751.
[7] K. Tachibana, T. Someya, Y. Arakawa, Appl. Phys. Lett. 74 (1999) 383.
[8] C. Adelmann, J. Simon, G. Feuillet, N.T. Pelekanos, B. Daudin, Appl. Phys. Lett. 76 (2000) 1570.
[9] L.W. Ji, Y.K. Su, S.J. Chang, L.W. Wu, T.H. Fang, J.F. Chen, T.Y. Tsai, Q.K. Xue, S.C. Chen, J. Cryst. Growth 249 (2003) 144.
[10] L.W. Ji, Y.K. Su, S.J. Chang, L.W. Wu, T.H. Fang, Q.K. Xue, W.C. Lai, Y.Z. Chiou, Mater. Lett. 57 (2003) 4218.
[11] S. Nakamura, K. Kitamura, H. Umeya, A. Jia, M. Kobayashi, A. Yoshikawa, M. Shimotomai, Y. Kato, K. Takahashi, Electron. Lett. 34 (1998) 2435.
[12] K. Tachibana, T. Someya, Y. Arakawa, Appl. Phys. Lett. 75 (1999) 2605.
[13] K. Tachibana, T. Someya, Y. Arakawa, IEEE J. Sel. Top. Quant. 6 (2000) 475.
[14] C. Winnewisser, J. Schneider, M. Börsch, H.W. Rotter, J. Appl. Phys. 89 (2001) 3091.
[15] L.W. Ji, Y.K. Su, S.J. Chang, C.S. Chang, L.W. Wu, W.C. Lai, X.L. Du, H. Chen, J. Cryst. Growth 263 (2004) 114.
[16] D.A.B. Miller, D.S. Chemla, T.C. Damen, A.C. Gossard, W. Wiegmann, T.H. Wood, C.A. Burrus, Phys. Rev. Lett. 53 (1984) 2173.
[17] D.A.B. Miller, D.S. Chemla, T.C. Damen, Phys. Rev. B 33 (1986) 6976.
[18] M. Klingenstein, J. Kuhl, J. Rosenzweig, C. Moglestue, A. Hulsmann, J. Schneider, K.K. Ohler, Solid State Electron. 37 (1994) 333.